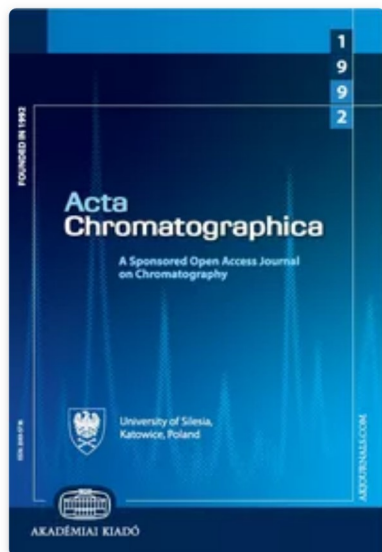




This site uses *cookies*, tags, and tracking settings to store information that help give you the very best browsing experience.





Acta Chromatographica

Online ISSN: 2083-5736

Acta Chromatographica

Volume/Issue: Volume 31: Issue 1

UPLC, HR-MS, and in-silico tools for simultaneous separation, characterization, and in-silico toxicity prediction of degradation products of atorvastatin and olmesartan

CHECK FOR UPDATES

Authors: [U. Rakibe, ...](#)

VIEW MORE +

Pages: 33–44

Online Publication Date: Mar 2019

Publication Date: 01 Mar 2019

Article Category: Research Article

DOI: [https://](https://doi.org/10.1556/1326.2017.00333)

doi.org/10.1556/1326.2017.00333

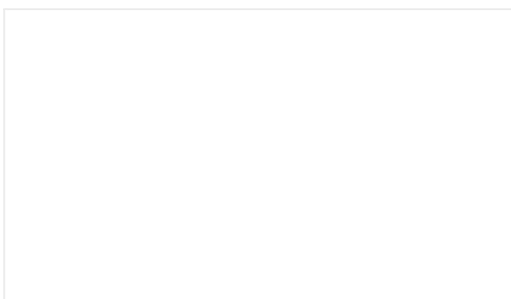
Abstract

The aim of this work was to simultaneously separate, identify, and characterize all the degradation products (DPs) of atorvastatin (AT) and olmesartan (OM) formed under different stress conditions as per International Conference on Harmonization (ICH) Q1A(R2) guideline. AT showed labile behavior in acidic, basic, neutral, and oxidative stress and led to the formation of two DPs, while OM degraded under acidic, basic, and neutral and resulted in the formation of four DPs. All the stressed samples of AT and OM were resolved on a C-18 column in single run on a gradient liquid chromatographic (LC) mode. A complete mass fragmentation pathway of both the drugs was established with the help of tandem mass spectrometry (MS/MS) studies. The fragmentation was further supported by MSⁿ studies, and for AT, it was carried out up to MS⁶, while for OM, it was up to MS⁵. Then, the stressed samples were analyzed by LC-MS/MS to get the fragmentation patterns of DPs. LC-MS/MS data helped to propose chemical structure of all the DPs. Based on this entire information, degradation pathway of both the drugs was established. The developed method has shown excellent linearity over the range of 10 to 150 µg/mL of OM and AT. The correlation coefficient (r^2) for OM and AT is 0.999 and 0.998, respectively. The main recovery value of OM and AT ranged from 99.97% to 100.54%, while the limit of detection (LOD) for OM and AT was 0.018 and 0.021 µg/mL, and limit of quantitation (LOQ) was found to be 0.051 and 0.063 µg/mL. Finally, the in-silico carcinogenicity, mutagenicity, and hepatotoxicity predictions of AT, OM, and all the DPs were performed by using toxicity prediction softwares, viz., TOPKAT,

LAZAR, and Discovery Studio ADMET, respectively.

Introduction



Atorvastatin (AT) is 3-hydroxy-3-methylglutaryl-coenzyme A (HMG-CoA) reductase inhibitors. Chemically, AT is (3*R*, 5*R*)-7-[2-(4-fluorophenyl)-3-phenyl-4-(phenylcarbamoyl)-5-propan-2-ylpyrrol-1-yl]-3,5-dihydroxyheptanoic acid (Figure 1a). It is the most effective and well-tolerated agent for treatment of dyslipidemia and can significantly reduce triglycerides levels used by elevated very low-density lipoprotein (VLDL) levels. Chemically, olmesartan (OM) is (5-methyl-2-oxo-2*H*-1,3-dioxol-4-yl)methyl 4-(2-hydroxypropan-2-yl)-2-propyl-1-({4-[2-(2*H*-1,2,3,4-tetrazol-5-yl)phenyl]phenyl)methyl)-1*H*-imidazole-5-carboxylate (Figure 1b). It is a non-peptide, orally active angiotensin receptor antagonists, which blocks the binding of angiotensin II to the AT1 receptor in vascular smooth muscles for treating hypertension. There exist few generic products in the market comprising AT and OM in solid oral dosage form, and moreover, drug interaction between the two drug substances is also not reported in the literatures. This type of dosage forms is usually recommended as a chronic therapy, and hence, the therapeutic concentration of AT and OM in systemic concentration is considered as one of the crucial factor to control the cardiovascular complications. Hence, it was thought worthwhile to develop an ultra-performance liquid chromatography (UPLC) and high-resolution mass spectrometry (HR-MS) method which can simultaneously separate, quantify, and characterize the degradation products of AT and OM.



 VIEW FULL SIZE

Figure 1.
Structure of atorvastatin (a) and
olmesartan (b)

Citation: *Acta Chromatographica Acta
Chromatographica* 31, 1;
[10.1556/1326.2017.00333](https://doi.org/10.1556/1326.2017.00333)

 [Download Figure](#)
 [Download figure as
PowerPoint slide](#)

There exist reports on reversed-phase high-performance liquid chromatographic (RP-HPLC) methods for simultaneous estimation of AT and OM by using HPLC and derivative spectroscopy [1, 2]. The literature search also revealed the existence of reports on simultaneous determination of AT and OM along with other drugs by HPLC and liquid chromatography–tandem mass spectrometry (LC–MS/MS) in human plasma [3–6]. Moreover, there are reports available on synthesis and characterization of process-related impurities of olmesartan medoxomil [7, 8]. AT is also reported for the determination of its impurities in bulk drug and tablets by HPLC and LC–MS [9–11].

However, there exists no comprehensive report or articles on the simultaneous separation and characterization of DPs of AT and OM by LC–MS analysis. Hence, the ultimate objective of our study was to (1) degrade both the drugs (AT and OM) under the conditions specified in Q1A(R2) guideline [12], (2) resolve the DPs generated on an HPLC column, (3) characterize them by LC–MS/MS studies, (4) postulate the degradation pathway for the drugs based on the stress degradation behavior, and, (5) finally, predict in-silico carcinogenicity, mutagenicity, and hepatotoxicity of drugs and DPs by using in-silico toxicity software's.

Experimental

Chemicals and Reagents

The drug substances (AT and OM) were received as gratis samples from Macleods Pharmaceutical Laboratories (Mumbai, India) and were used without further purification. Analytical reagent (AR) grade hydrochloric acid (HCl) and HPLC grade methanol (MeOH) were purchased from Merck Specialities Pvt. Ltd. (Mumbai, India). AR grade sodium hydroxide (NaOH) was purchased from S.D. Fine-Chem Ltd. (Mumbai, India), and hydrogen peroxide (H₂O₂) was purchased from Qualigens Fine Chemicals Pvt. Ltd. (Mumbai, India). Ultra-pure HPLC grade water was obtained from Millipore water purification system (Molsheim, France).

Equipment

A high-performance liquid chromatography (HPLC) system from PerkinElmer (Shelton, CT, USA) was used for the LC studies, which consisted of an on-line degasser, a sample injector (Rheodyne sample loop 20 mL), a ultraviolet (UV)-visible detector (Series 200), a pump (Reciprocating, series 200), and a computer system loaded with Total Chrome Navigator (version 6.3.1) software. The LC-MS system was controlled by Xcalibur software (version 2.0) consisted of LCQ Fleet and TSQ Quantum Access with Surveyor Plus HPLC System (Thermo, San Jose, USA). Precision water baths equipped with MV controller (Thermostatic Classic Scientific India Ltd. Mumbai, India) 90 were used for stress studies. Degradation experiments in acid, base, and neutral conditions were performed using a dry-bath (Labline Sun Scientifics Ltd. New Delhi, India). The solid state thermal stress studies were carried out in dry-air oven (NSW Limited, New Delhi, India). Other equipment used was a micro-pipette (Erba Biohit, Mannheim, Germany), a weighing balance (Shimadzu, AUX220, Kyoto, Japan), and a pH meter (Labindia, Mumbai, India). All the separations were achieved on a C-18 Kromasil column (Eka Chemicals AB, Bohus, Sweden). Photolytic studies were

carried out in a photostability chamber (Thermolab, 95 Th-400G Mumbai, India), set at 40 ± 1 °C/ $75\% \pm 3\%$ RH, consisting of a combination of black UV lamps and white fluorescent lamps as per ICH guideline Q1B [13]. The in-silico toxicity softwares, viz., TOPKAT (BIOVIA, San Diego, USA) and Lazar (In Silico Technologies gmbh, Basel, Switzerland), were used for prediction of carcinogenicity, while hepatotoxicity study was performed by Discovery Studio (BIOVIA, San Diego, USA).

Stress Studies

As per the ICH Q1A(R2) guideline, the stress degradation studies were conducted under hydrolytic, photolytic, oxidative, and thermal conditions. The stock solution of drugs was prepared in methanol at the concentration of 2000 µg/mL. The stressor (e.g., HCl, NaOH, H₂O₂) and the drug solution were used in 50:50 v/v under all the stress conditions. The initial stress degradation experiments were conducted by adopting lower concentration of stressors and lower temperature to optimize the stress conditions as well as to achieve 5–15% degradation in respective stress conditions. In the initial acid stress experiments, both the drug substances (AT and OM) showed high degradation (above 20%) at 1 N HCl; hence, the concentration of acid was gradually decreased to get optimum degradation, while in alkali stress experiments, both the drug substances showed different stability behavior. The alkaline stressor (NaOH) was increased from lower concentration to higher concentration for AT, while for OM, the alkaline stressor concentration was decreased and set at 0.05 N to achieve optimum degradation. The oxidative stress conditions were optimized from lower hydrogen peroxide concentration (0.3%) to higher concentration (15%). The photolytic and thermal stress conditions were set as same for both the drug substances. For AT, acid, base, and neutral hydrolysis were carried out by heating in 0.1 N HCl, 2 N NaOH and water at 80 °C for 1 h, 2 h, and 1

h, respectively. The potential for oxidative decomposition was studied in 15% H₂O₂ at room temperature for 48 h. For OM, acid, base, and neutral hydrolyses were carried out by heating in 0.1 N HCl, 0.05 N NaOH, and water at 80 °C for 2 h, 1 h, and 1 h, respectively. The oxidative study was carried out in 15% H₂O₂ at room temperature for 48 h. Thermal experiments were performed by sealing drugs in glass vials and placed in dry oven at 50 °C for 21 days. Photolytic studies were carried out by exposing the thin layer of both the drugs separately in a photostability chamber set at accelerated conditions (40 ± 1 °C /75% ± 3% RH). The optimized stress conditions for AT and OM are shown in Tables 1a and 1b, respectively.

Table 1a.
Stress conditions for optimum degradation of atorvastatin

Stress condition	Concentration of stressor	Exposure time and temperature
Hydrolysis Acid	0.1 N HCl	
Neutral	H ₂ O	80 °C
Base	2 N NaOH	
Oxidation	15% H ₂ O ₂	RT
Photolysis	8500 Lx. h fluorescent and C	
Acid	0.01 N HCl	
Neutral	H ₂ O	40 °C
Base	0.01 N NaOH	75% F
Solid	–	
Thermal	–	50 °C

Table 1b.
Stress conditions for optimum
degradation of olmesartan

Stress condition	Concentration of stressor	Exposure concentration
Hydrolysis Acid	0.1 N HCl	
Neutral	H ₂ O	80 °C
Base	0.05 N NaOH	
Oxidation	15% H ₂ O ₂	RT
Photolysis	8500 Lx. h fluorescent and C	
Acid	0.01 N HCl	
Neutral	H ₂ O	40 °C
Base	0.01 N NaOH	75% F
Solid	–	
Thermal	–	50 °C

Samples Preparation for HPLC Analysis

The stressed samples of AT and OM were withdrawn at suitable time intervals stated in the optimized stress conditions and diluted further with water methanol (95:5, v/v) to get the final concentration of 100 µg/mL before injecting into HPLC system.

HPLC Method Development

Both the drugs were scanned from 200 nm to 400 nm at the concentration of 10 µg/mL individually, and overlay spectra revealed that 256 nm was the wavelength showing maximum absorbance, and hence, it was selected for further analysis. To achieve an adequate separation, different proportion of potassium dihydrogen phosphate buffer with methanol and pH was varied using orthophosphoric acid.

Initially, a gradient HPLC method was developed to separate pure AT and OM in order to check the retention profile for both the drugs. Then, all the stressed solutions were injected individually into HPLC system. The method was optimized to separate all the DPs of both the drugs in the single run.

Mass Spectral Studies on Drugs

The drugs (AT and OM) were directly infused separately into the MS system at a concentration of 10 µg/mL prepared in methanol in positive mode using electrospray ionization (ESI) technique in the mass range of 50–800 Da. The MS operating parameters were suitably optimized to achieve adequate fragmentation of drugs; moreover, the origin of each fragment was obtained by subjecting drugs to multi-stage (MS^n) mass studies. Different collision energy was applied to achieve the fragmentation of precursor ions. The MS fragments of AT and OM are listed in Tables 2 and 3, respectively.

Table 2.
Interpretation of MS data of
fragments of atorvastatin

Peak no.	Experimental mass	Best possible molecular formulae
1	559.36	$C_{33}H_{36}N_2O$
2	536.72	$C_{33}H_{29}N_2O$
3	466.27	$C_{27}H_{29}NO_5$
4	448.24	$C_{27}H_{27}NO_4$
5	440.46	$C_{26}H_{31}NO_4$
6	430.22	$C_{27}H_{25}NO_3$
7	422.24	$C_{26}H_{29}NO_3$

Peak no.	Experimental mass	Best possible molecular formulae
8	388.43	C ₂₆ H ₂₇ NOF
9	370.11	C ₂₆ H ₂₈ NO ⁺
10	344.20	C ₂₄ H ₂₆ NO ⁺
11	341.18	C ₂₀ H ₂₃ NO ₄
12	320.09	C ₂₁ H ₁₉ NOF
13	302.22	C ₂₁ H ₂₀ NO ⁺
14	294.25	C ₂₀ H ₂₁ NF ⁺
15	288.13	C ₂₀ H ₁₈ NO ⁺
16	276.30	C ₁₉ H ₁₅ NF ⁺
17	243.26	C ₁₆ H ₂₁ NO ⁺
18	180.76	C ₁₁ H ₁₅ NF ⁺
19	84.99	C ₅ H ₁₀ N ⁺

RDB: ring plus double bonds

Table 3.
Interpretation of MS data of
fragments of the olmesartan

Peak no.	Experimental mass	Best possible molecular formulae
1	559.15	C ₂₉ H ₃₁ N ₆ O
2	541.19	C ₂₉ H ₂₉ N ₆ O
3	513.24	C ₂₇ H ₂₅ N ₆ O
4	447.21	C ₂₆ H ₂₇ N ₂ O

Peak no.	Experimental mass	Best possible molecular formulae
5	429.22	C ₂₅ H ₂₁ N ₂ O
6	401.22	C ₂₂ H ₂₉ N ₂ O
7	319.21	C ₂₁ H ₂₃ N ₂ O
8	235.13	C ₁₆ H ₁₅ N ₂ ⁺
9	207.15	C ₁₄ H ₁₁ N ₂ ⁺
10	195.09	C ₁₄ H ₁₃ N ⁺
11	179.15	C ₁₃ H ₉ N ⁺
12	121.05	C ₇ H ₇ NO ⁺

RDB: ring plus double bonds

LC–MS Analysis

The stressed samples were subjected to LC–MS analysis to study the mass fragments of each DP and finally to assign structures to them. The initially developed gradient LC method was used during the LC–MS analysis of stressed samples of both the drugs; however, buffer component (phosphate) was replaced by MS compatible buffer ammonium acetate. All the DPs were identified with the help of LC–MS fragmentation analyses. The masses of all DPs of AT and OM, generated in LC–MS studies, are shown in Table 4.

Table 4.
LC–MS/MS data of DPs of atorvastatin (AT) and olmesartan (OM) along with their possible molecular formulae and major fragments

DPs	Experimental mass	Best possible
-----	-------------------	---------------

		molecular formula
AT-1	541.33	$C_{33}H_{34}N_2O_4$
AT-2	573.33	$C_{33}H_{34}N_2O_6$
OM-1	461.17	$C_{25}H_{29}N_6O_3$
OM-2	447.17	$C_{24}H_{27}N_6O_3$

OM-3	452.92	$C_{25}H_{28}N_2O_6$
------	--------	----------------------

RDB: ring plus double bonds

In-Silico Toxicity Studies

The drugs and all degradation products were subjected to in-silico carcinogenicity, mutagenicity, and hepatotoxicity predictions by using different models. Carcinogenicity and mutagenicity predictions were performed by using TOPKAT (Toxicity Prediction by Komputer Assisted Technology) version 6.2 and Lazar toxicity prediction software version 1.1.2 built on top of the OpenTox framework and adopting DSSTox database. TOPKAT and Lazar carcinogenicity prediction softwares provide statistically qualified data with respect to male and female mouse and rat models. Hepatotoxicity prediction was carried out by using Discovery Studio ADMET. The model was developed from available literature data of 382 compounds known to exhibit liver toxicity or trigger dose-related elevated aminotransferase levels in more than 10% of the human population [14].

Results and Discussion

LC Method Development

An HPLC analysis of individual reaction solutions of AT and OM revealed the overlapping of polar DPs on polar sides of both the drugs. The method was optimized by analyzing degraded drug samples and changing the individual method parameters one after another to assess the impact of change on method efficiency. As shown in

Figure 2, an acceptable separation was achieved using MeOH (A): ammonium acetate buffer (B) (0.01 M, pH 5 with acetic acid) in a gradient mode: $T_{\min}/A:B$, $T_0/10:90$, $T_5/10:90$, $T_{15}/50:50$, $T_{20}/65:35$, $T_{30}/80:20$, $T_{32}/10:90$, and $T_{35}/10:90$. The detection was carried out at 256 nm; flow rate was 1 mL/min, and injection volume was 20 μ L.


 VIEW FULL SIZE

Figure 2.

Chromatogram showing separation of degradation products (OM1, OM2, OM3, OM4, and AT1, AT2) and drug (OM and AT) in the mixture of stress samples. Key: A: acid; B: base; N: neutral; O: oxidative

Citation: *Acta Chromatographica Acta Chromatographica* 31, 1;
[10.1556/1326.2017.00333](https://doi.org/10.1556/1326.2017.00333)

 [Download Figure](#)

 [Download figure as PowerPoint slide](#)

Degradation Behavior of Drugs

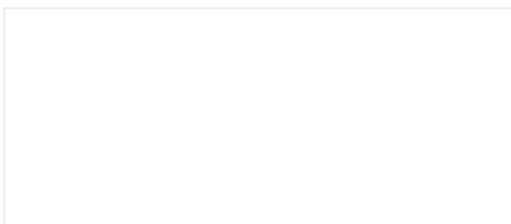
The primary degradation products of AT are AT1 and AT2, while a total of four DPs such as OM1, OM2, OM3, and OM4 were formed by OM. AT1 was formed in acidic, alkaline, and neutral stress conditions, while AT2 was formed in acid and oxidative stress conditions. OM1, OM2, OM3, and OM4 were formed in acidic condition, while OM1, OM2, and OM3 were formed as common DPs under alkaline and neutral conditions. Both the drugs (AT and OM) were found to be stable in all other stress conditions including thermal and photolytic

conditions. The degradation behavior of AT and OM is shown in Figure 2, where the DPs are denoted as OM1 to OM4 and AT1 to AT2 as per the peaks elution from left to right in the chromatogram.

Mass Fragmentation Behavior of AT and OM

Mass spectrum of the AT and OM obtained from MS and MSⁿ studies is shown in Figures 3 and 4, respectively. The most probable formula for the fragments was calculated using elemental composition calculator. Multi-stage MSⁿ studies were carried out to understand the origin of each fragment formed during MS analysis. Moreover, the objective behind conducting MSⁿ experiments was to confirm the fragments obtained in MS studies after application of collision energy and to assign the correct structure to each fragment, which is an effective tool to propose an accurate fragmentation pathway. The MSⁿ experiments also supported in establishing the chemistry of fragments of standard drug substances (AT and OM) after application of excess of collision energy, which may not be necessarily identical with the degradation pathway of degradation products, due to difference in collision energy induced bond cleavages and forced degradation reaction conditions. The optimized MS operating parameters such as collision energy M + H – 5 eV/z and fragments –11 eV/z, transfer time M + H 45 (μs) and fragments 38 (μs), collision RF M + H – 220 (Vpp) and fragments 170 (Vpp), and pre-pulse storage applicable M + H 5 (μs) and fragments 5 (μs) were used to obtain molecular ion peak and possible fragments of AT and OM. A total of 6 fragments were generated from AT, and 11 fragments were generated from OM, while the molecular ion peak of AT (559.36) and OM (559.15) is shown as 0. Parent ion having a mass of *m/z* 559.36 followed three different pathways on loss of C₆H₇N (~93.06 Da), C₇H₇NO (~121.05 Da), and H₂O (~22.67 Da) and led to the formation of fragments with *m/z* 466.20,

440.22, and 536.59, respectively. The fragment with m/z 466.20 on cyclization and loss of water molecule resulted in the formation of a daughter ion with m/z 448.19, which followed a separate parallel fragmentation pathway. The ion with m/z 448.19 on cleavage of a water molecule and tetrahydro-4-hydroxy-6-methylpyran-2-one led to the formation of daughter ions with m/z 430.18 and m/z 320.14, respectively. The daughter ion fragment of m/z 320.14 on loss of a methyl group and a carbonyl group of pyrrole ring resulted in the formation of a fragment with m/z 276.11. The ion with m/z 430.18 on loss of a formic acid moiety produced a daughter ion of m/z 388.20, whereas the fragment m/z 388.20 on cleavage of fluorine and pent-2-ene moiety resulted in the formation of ions with m/z 370.12 and m/z 302.12, respectively. The ion with m/z 302.12 on loss of a methyl group and ion with m/z 370.12 on loss of an ethylene moiety led to the formation of fragments with m/z 288.13 and m/z 344.20, respectively. A major fragment ion with m/z 440.22 underwent a parallel fragmentation pathway and produced ions with m/z 341.16 and m/z 422.21 on loss of fluorobenzene and a water molecule, respectively. A loss of tetrahydro-4-hydroxy-6-methylpyran-2-one from ion with m/z 422.21 produced a fragment with m/z 294.16, while ion with m/z 341.16 on cleavage of 3-hydroxy butanoic acid moiety resulted in the formation of daughter ion with m/z 243.16. The fragment with m/z 294.16 on loss of a propyl group resulted in the formation of fragment with m/z 180.11, while the ion m/z 180.11 underwent a loss of fluorobenzene moiety and led to the formation of daughter ion with m/z 84.08. The proposed structures of the fragments and pathway are shown in Figure 5.




 VIEW FULL SIZE

Figure 3.
Line spectrum of atorvastatin
obtained in MS and MSⁿ study

Citation: Acta Chromatographica Acta
Chromatographica 31, 1;
[10.1556/1326.2017.00333](https://doi.org/10.1556/1326.2017.00333)

 [Download Figure](#)


 [Download figure as
PowerPoint slide](#)

 VIEW FULL SIZE

Figure 4.
Line spectrum of olmesartan
obtained in MS and MSⁿ study

Citation: Acta Chromatographica Acta
Chromatographica 31, 1;
[10.1556/1326.2017.00333](https://doi.org/10.1556/1326.2017.00333)

 [Download Figure](#)

 [Download figure as
PowerPoint slide](#)

 VIEW FULL SIZE

Figure 5.
Mass fragmentation pattern of
atorvastatin

Citation: Acta Chromatographica Acta
Chromatographica 31, 1;
[10.1556/1326.2017.00333](https://doi.org/10.1556/1326.2017.00333)

[Download Figure](#)[Download figure as
PowerPoint slide](#)

A total of 11 fragments were formed from OM; among these, the molecular ion peak with m/z 559.15, 541.19, 447.21, 429.22, and 207.15 has shown good peak intensity, while the fragments with m/z 513.24, 401.22, 319.21, 235.13, 195.09, 179.15, and 121.05 had very less abundance. The molecular ion fragment of OM on loss of a water molecule led to the formation of daughter ion with m/z 541.21, which subsequently on cleavage of triazole ring and ethyl moiety resulted in the formation of fragments with m/z 401.20 and m/z 513.18. The fragment with m/z 447.19 was the product obtained from ion with m/z 513.18 on loss of triazole ring. The loss of a methyl group and two protons from m/z 447.19 resulted in the formation of ion with m/z 429.14, while the cleavage of 4-(hydroxymethyl)-5-methyl-1,3-dioxol-2-one from m/z 447.19 resulted in the formation of the ion with m/z 319.18, which underwent loss of biphenylmethanamine and resulted in the formation of fragment with m/z 121.05. The fragment with m/z 429.14 followed a separate parallel pathway, and structure of all the fragments is shown in Figure 6.

 VIEW FULL SIZE

Figure 6.
Mass fragmentation pattern of
olmesartan

Citation: Acta Chromatographica Acta
Chromatographica 31, 1;
[10.1556/1326.2017.00333](https://doi.org/10.1556/1326.2017.00333)

[Download Figure](#)[Download figure as
PowerPoint slide](#)

LC–MS Analysis of Stressed Samples

To elucidate the structure of each DP formed during stress studies, all the samples were analyzed in positive ESI mode of LC–MS system to establish the fragment profiles. Line spectra of degradation products of AT and OM obtained in LC–MS/MS studies are shown in Figures 7 and 8, respectively.

 VIEW FULL SIZE**Figure 7.**

Line spectra of degradation products (AT-1 and AT-2) of atorvastatin obtained in LC-MS/MS studies

Citation: *Acta Chromatographica Acta Chromatographica* 31, 1;
[10.1556/1326.2017.00333](https://doi.org/10.1556/1326.2017.00333)

[Download Figure](#)[Download figure as
PowerPoint slide](#) VIEW FULL SIZE**Figure 8.**

Line spectra of degradation products of olmesartan (OM-1,

OM-2, and OM-3) obtained in LC-MS/MS studies

Citation: *Acta Chromatographica Acta Chromatographica* 31, 1;
[10.1556/1326.2017.00333](https://doi.org/10.1556/1326.2017.00333)

[Download Figure](#)

[Download figure as PowerPoint slide](#)

Proposed Structures of DPs

The product AT1 has the molecular mass of m/z 541.26, which is 18 Da less than the molecular ion peak of AT. The molecule underwent cyclization to form lactone ester with the loss of a water molecule (18 Da). This transformation resulted in the formation of AT1. Another degradation product AT2 formed in acidic and oxidative conditions had a mass of m/z 573, which was 13.97 Da higher than AT (559); this suggested some additions in the drug rather than cleavage. It has been reported that the pyrrole ring is a good substrate for singlet oxygen attack at position 2,3 to form an epoxide intermediate. Then, the final product AT2 was formed by rearrangement of epoxide to form stable product with the subsequent migration of isopropyl moiety [11, 15].

The molecular mass difference between OM and OM1 is 98.01 Da; no moiety/group other than 4-methyl-1,3-dioxol-2-one can compensate this loss. Hence, it was concluded that 4-methyl-1,3-dioxol-2-one moiety of OM has undergone cleavage and resulted in the formation of OM1. A comparatively similar type of cleavage and loss of moiety was found in case of OM2 as well. The possibility of loss of 112.02 Da fragment from any other moiety of the drug (OM) was ruled out except 4,5-dimethyl-1,3-dioxol-2-one; hence, it was proposed that the loss of this moiety from OM resulted in the formation of OM2. A direct cleavage of tetrazole ring (69 Da) from the drug (OM) resulted in the formation of OM3, while loss



of 69 Da could not be compensated by any other groups present in the drug substance. The product OM4 could not be analyzed in positive or negative ESI mode, maybe due to its poor ionizability. The proposed structures and schemes for all the degradation products of AT1 and AT2 are depicted in Figures 9 and 10, respectively, while fragmentation pathway for OM1, OM2, and OM3 is shown in Figure 11, respectively. Furthermore, the degradation pathways for both the drugs (AT and OM) are shown in Figures 12 and 13.



 VIEW FULL SIZE

Figure 9.
Fragmentation pathway of AT-1

Citation: *Acta Chromatographica Acta Chromatographica* 31, 1;
[10.1556/1326.2017.00333](https://doi.org/10.1556/1326.2017.00333)

 [Download Figure](#)
 [Download figure as PowerPoint slide](#)



 VIEW FULL SIZE

Figure 10.
Fragmentation pathway of AT-2

Citation: *Acta Chromatographica Acta Chromatographica* 31, 1;
[10.1556/1326.2017.00333](https://doi.org/10.1556/1326.2017.00333)

 [Download Figure](#)

[Download figure as PowerPoint slide](#)

 VIEW FULL SIZE

Figure 11.
Fragmentation pathway of OM-1,
OM-2, and OM-3

Citation: Acta Chromatographica Acta Chromatographica 31, 1;
[10.1556/1326.2017.00333](https://doi.org/10.1556/1326.2017.00333)

[Download Figure](#)
[Download figure as PowerPoint slide](#)

 VIEW FULL SIZE

Figure 12.
Degradation pathway of
atorvastatin

Citation: Acta Chromatographica Acta Chromatographica 31, 1;
[10.1556/1326.2017.00333](https://doi.org/10.1556/1326.2017.00333)

[Download Figure](#)
[Download figure as PowerPoint slide](#)

 VIEW FULL SIZE

Figure 13.
Degradation pathway of
olmesartan

Citation: *Acta Chromatographica Acta Chromatographica* 31, 1;
[10.1556/1326.2017.00333](https://doi.org/10.1556/1326.2017.00333)

[Download Figure](#)
[Download figure as
PowerPoint slide](#)

Method Validation

The described method was validated with respective specificity, precision, intermediate precision, linearity, LOD and LOQ, and recovery.

Specificity

Specificity of the method was evaluated by injecting blank solution (diluent), individual OM and AT 100 µg/mL solution, and mixture of both the solutions. In specificity study, all degradation product of both analytes was separated and no interference of degradation products was observed. The retention time of OM and AT was found to be 22.3 and 25.8, respectively, while tailing factors for OM and AT were recorded as 1.15 and 1.52, respectively. The other parameters such as resolution between OM and AT were found to be 5.5, while theoretical plates for OM and AT were found to be 8995 and 9820, respectively. The system suitability parameters are shown in Table 5.

Table 5.
System suitability, regression,
precision, and recovery parameters of
OM and AT

Parameters	OM	AT
Retention time	22.3	25.8

Parameters	OM	AT
Tailing factors	1.15	1.41
Resolution	–	5.2
Theoretical plates	8995	9820
Limit of detection (LOD), µg/mL	0.018	0.021
Limit of Quantitation (LOQ), µg/mL	0.051	0.063
Slope (m)	1580.8	7956.3
Intercept (C)	1627.4	2146.3
Correlation coefficient (<i>r</i>)	0.999	0.998
Method precision (% RSD)	0.66	0.75
Intermediate precision (% RSD)	0.98	0.88
Recovery (%)	99.97	100.54

Precision

The method precision was studied by injecting six injections of 100 µg/mL mixture of both AT and OM solution. The area % relative standard deviation (RSD) was calculated. The area % RSD for OM and AT was found to be 0.66 and 0.75, respectively, while the results are shown in Table 5.

Intermediate Precision

Intermediate precision of the method was studied by injecting six injection of 100 µg/mL mixture of both AT and OM solution with different analyst, different system and

on different day. The area % RSD was calculated. The area % RSD for OM and AT was found to be 0.98 and 0.88, respectively. The intermediate precision results are depicted in Table 5.

Linearity

Linearity of the method was tested from 10% to 150% of 100 µg/mL of both the analytes OM and AT. Mixed standard solution 10, 20, 40, 60, 80, 90, 100, 110, 120, 130, and 150 µg/mL of OM and AT was injected in triplicate. The calibration plot was obtained by plotting peak area verses concentration. The equation of the calibration curve for OM and AT was $Y = 1580.8x - 1627.4$ and $Y = 7956.3x + 2146.3$, respectively. The linearity results are depicted in Table 5.

LOD and LOQ

LOD and LOQ for OM and AT were determined by linearity curve by using slope and intercept. The LOD for OM and AT was 0.018 and 0.021 µg/mL, respectively, while LOQ levels were 0.051 and 0.063 µg/mL. The results of LOD and LOQ are shown in Table 5.

Accuracy/Recovery

The recovery of the method was performed by adding known amount of drug in blank. The recovery was performed at three levels, 50%, 100%, and 150% of 100 µg/mL concentration. The recovery values are shown in Table 5.

Robustness

The robustness of the method was performed by making the deliberate variations in following chromatographic parameters. The flow rate of mobile phase was 1.0 mL/min; to study the effect of flow rate on resolution between OM, OM4, and AT, it was changed to 0.1 units from 1.0 to 1.1 mL/min and 0.9 mL/min. The effect of column temperature on resolution was also studied at 28 °C and 32 °C. The resolution between OM, OM4, and AT was not less than 5.0 in the robustness study.

Results of In-silico Toxicity Studies

The carcinogenicity results obtained from TOPKAT and Lazar toxicity model software revealed that AT, AT1, AT2, OM, and OM3 were found to be carcinogenic, while OM1 and OM2 were non-carcinogenic. As per TOPKAT model assessment, the values below 0.3 indicate non-carcinogen and above 0.7 signify carcinogen, while the values between 0.3 to 0.7 are considered in intermediate zone. All the compounds under investigation (Drug and DPs) except AT2 were found to be mutagen (active) as per Lazar toxicity prediction model. The results obtained in hepatotoxicity study by using Discovery Studio ADMET model revealed that the AT, AT1, and AT2 were found to be hepatotoxic, while OM and all its DPs were non-toxic. The computed probability for toxic and non-toxic values as per Discovery Studio ADMET is 0.5 or less and 0.5 or more, respectively. However, the results obtained for AT (0.629), AT1 (0.735), and AT2 (0.629) indicate high probability of hepatotoxic potential. The in-silico toxicity determination is a type of theoretical prediction about toxic or non-toxic behavior of drug substance and degradation products, but these values alone may not be safety impacting factor. Hence, in-silico toxicity predictions need an additional confirmatory support by in vivo toxicity studies to declare the molecules inherent toxic or non-toxic behavior. The in-silico carcinogenicity and hepatotoxicity results are depicted in Table 6.

Table 6.
In-silico carcinogenicity, mutagenicity,
and hepatotoxicity study data of drug
and DPs

Drug/ DPs	Carcinogenicity	
	TOPKAT	Lazar toxicity
AT	0.931 (Carcinogen)	Carcinogen

Drug/ DPs	Carcinogenicity	
	TOPKAT	Lazar toxicity
AT-1	0.915 (Carcinogen)	Carcinogen
AT-2	0.851 (Carcinogen)	Carcinogen
OM	1.000 (Carcinogen)	Carcinogen
OM-1	0.028 (Non- carcinogen)	(Non- carcinogen)
OM-2	0.000 (Non- carcinogen)	(Non- carcinogen)
OM-3	1.000 (Carcinogen)	Carcinogen

Conclusions

The study was able to yield new and useful information, yet not reported in the literature on simultaneous separation of AT and OM, as well as their degradation products by RP-HPLC method. Moreover, the major focus of the study was to characterize and propose structures of all the degradation products of AT and OM by MS, MSⁿ, and LC-MS/MS techniques and to validate the LC separation method. The developed HPLC method was found to be suitable for separation of all the DPs formed under the specified stress conditions. For AT, the product AT1 was the result of acid, alkaline, and neutral hydrolysis, while AT2 was formed as common DP under acidic and oxidative stress conditions. For OM, the products OM1, OM2, OM3, and OM4 were formed as a result of acid hydrolysis, whereas OM1, OM2, and OM3 were common for acidic, alkaline, and neutral stress conditions, respectively. The degradation pathway for both the drugs was postulated with the

help of the MSⁿ studies, while the DPs were identified and characterized with the help of data obtained during MSⁿ and LC–MS/MS analysis. In line with the reported method, for the first time, we developed a simultaneous separation, identification, structure elucidation, and validation of combined OM and AT different from the reported methods. Advantages of this method over existing methods are that it can be used in quality control department and stability study of combination products containing atorvastatin and olmesartan. Moreover, the developed LC–MS compatible method can be used for biological analysis of both the drugs in combination in a single run. The in-silico toxicity study revealed the carcinogenic potential of AT, AT1, AT2, and OM, while, except AT2, all the compounds were found to be mutagenic. Finally, as per Discovery Studio, AT, AT1, and AT2 were declared to be hepatotoxic based on higher scores.

References

1. ↑ Mhaske, R. A.; Sahasrabudhe, S.; Mhaske, A. A.; Garole, D. J. *Int. J. Pharm. Sci. Res.* 2012, 3, 793.

[Search Google Scholar](#)

[Export Citation](#)

2. ↑ Patel, N. N.; Patel, P. R.; Tandel, F. A.; Kothari, C. S.; Shah, S. A. *Int. J. Pharm. Pharm. Sci.* 2000, 5, 1.

[Search Google Scholar](#)

[Export Citation](#)

3. ↑ Gajula, R.; Pilli, N. R.; Ravi, V. B.; Maddela, R.; Inamadugu, J. K.; Polagani, S. R.; Busa, S. *Sci. Pharm.* 2012, 80, 923.

[Crossref](#)

[Search Google Scholar](#)

[Export Citation](#)

4. Altuntas, T. G.; Erk, N. *J. Liq. Chromatogr. Rel. Technol.* 2004, 27, 83.

[Crossref](#) |
[Search Google Scholar](#) |
[Export Citation](#)

5. Liu, D.; Jiang, J.; Wang, P.; Feng, S.;
Hu, P. *J. Chromatogr. B* 2010, 878,
743.

[Crossref](#) |
[Search Google Scholar](#) |
[Export Citation](#)

6. ↑ Hotha, K. K.; Yarramu, N. R.;
Kandibedala, T.; Dasari, V. B.;
Vobalaboina, V. *Am. J. Anal. Chem.*
2012, 3, 559.

[Crossref](#) |
[Search Google Scholar](#) |
[Export Citation](#)

7. ↑ Venkanna, G.; Madhusudhan, G.
G.; Mukkanti, K.; Sankar, A.; Sampath
Kumar, Y.; Venakata Narayana, Y. G. *J.*
Chem. 2013, 2013, 1.

[Crossref](#) |
[Search Google Scholar](#) |
[Export Citation](#)

8. ↑ Babu, K. S.; Tagore, A. R.; Reddy,
G. S.; Venkateswarlu, G.; Reddy, P. P.;
Anand, R. V. *ARKIVOC* 2010, 2010. 2,
392.

[Search Google Scholar](#) |
[Export Citation](#)

BROWSE TITLES

SUBJECTS

SUBSCRIPTIONS

FREQUENTLY ASKED QUESTIONS

FOR AUTHORS

LIBRARIANS

ABOUT US

JOURNALS

[TERMS OF USE](#)[PRIVACY POLICY](#)[CONTACT US](#)[NEWSLETTER](#)[OUR BLOG](#)[AKADEMIAI.HU](#)[SCIENTIFIC CONFERENCES](#)[ONLINE DICTIONARY](#)

Copyright Akadémiai Kiadó

AKJournals is the trademark of Akadémiai Kiadó's journal publishing business branch.

Access brought to you by:
Dr. Babasaheb Ambedkar
Marathwada University

Powered by PubFactory

15. ↑ Vukkum, P.; Babu, J. M.;
Murlikrishna, R. *Sci. Pharm.* 2013, 81,
93.

[Crossref](#)

[Search Google Scholar](#)

[Export Citation](#)